Dominance of Long-Lived Excitations in the Antiferromagnetic Spin-1 Chain NENP

Shaolong Ma,[1] Collin Broholm,[1,3] Daniel H. Reich,[1]
B. J. Sternlieb,[2,a] and R. W. Erwin[3]
[1]*Department of Physics and Astronomy, Johns Hopkins University, Baltimore, Maryland 21218*
[2]*Department of Physics, Columbia University, New York, New York 10027*
[3]*National Institute of Standards and Technology, Gaithersburg, Maryland 20899*
(Received 19 June 1992)

We have measured the dynamic spin correlation function for the quasi-one-dimensional $S = 1$ antiferromagnet NENP by inelastic magnetic neutron scattering. Long-lived excitations ($\omega\tau > 10$) exist for $0.3\pi \leq \tilde{q} \leq \pi$, and within error exhaust the total moment sum rule. The dispersion relation retains the fundamental periodicity of the spin chain, explicitly demonstrating the absence of broken translational symmetry in the ground state. The instantaneous spin correlation function follows a square-root Lorentzian for $\tilde{q} \simeq \pi$ but deviates substantially from this form for $\tilde{q} < 0.8\pi$.

PACS numbers: 75.25.+z, 75.10.Jm, 75.40.Gb

The antiferromagnetic integer spin chain is among the few quantum many-body systems with a finite two-point correlation length at $T = 0$ K. Theory [1], numerical simulations [2], and experiment [3–10] have concentrated on understanding the excitation spectrum near $\tilde{q} = \pi$ where the Haldane gap Δ separates the singlet ground state from the excited triplet and near $\tilde{q} = 0$ where it is believed that a multimagnon continuum exists above a gap 2Δ corresponding to the creation of two counterpropagating $\tilde{q} = \pi$ magnons [11–13]. For general $\tilde{q}$ much less is known, even about the qualitative features of the spectrum.

We have therefore measured the excitation spectrum for $0 \leq \tilde{q} \leq \pi$ in the quasi-one-dimensional $S = 1$ system $Ni(C_2H_8N_2)_2NO_2ClO_4$ (NENP). We find that the dynamic spin correlation function $\mathcal{S}(\tilde{q},\omega)$ is dominated by one-magnon-like resonant modes that follow a dispersion relation with fundamental periodicity in $\tilde{q}$ of 2π and that these excitations are well described by the single mode approximation (SMA). This work is the first complete experimental study of the excitation spectrum of a quantum spin liquid.

A number of neutron scattering experiments in 1D $S = 1$ antiferromagnets have already been published [3, 4, 10]. Most relevant for our work are experiments by Tun *et al.* on $CsNiCl_3$ that show broad peaks in the excitation spectrum with a 2π periodicity in $\tilde{q}$ [3]. These results were obtained in the quasi-one-dimensional phase of this material at $k_BT/\Delta = 0.6$.

Unlike $CsNiCl_3$, NENP apparently does not undergo three-dimensional ordering, and hence may be studied in the $T \sim 0$ K limit. NENP is described by a 1D Hamiltonian with planar anisotropy

$$\mathcal{H} = J\sum_{\ell} \mathbf{S}_\ell \cdot \mathbf{S}_{\ell+1} + D\sum_{\ell}(S^z_\ell)^2 , \qquad (1)$$

where $\hat{\mathbf{z}}$ is the chain axis, $J = 3.8$–4.1 meV, and $D = 0.2J$ [14, 15]. Its excitation spectrum has been well studied near $\tilde{q} = \pi$ [4] where planar anisotropy splits the triplet excitation into two modes with energies 1.2 and 2.4 meV for fluctuations perpendicular and parallel to the chain, respectively. These energies are modulated slightly by weak interchain coupling ($J'/J \simeq 10^{-4}$) [4], and the lower mode is split by 0.17 meV due to in-plane anisotropy [16].

NENP is orthorhombic with lattice parameters a =15.223 Å, b=10.300 Å, and c=8.295 Å [14]. We index momentum transfer in the corresponding reciprocal lattice $\mathbf{Q} = h\mathbf{a}^* + k\mathbf{b}^* + l\mathbf{c}^* \equiv (hkl)$, and since Ni atoms in a chain are separate by $\mathbf{b}/2$ we refer to wave vector transfer along the chain in terms of $\tilde{q} = \mathbf{Q}\cdot(\mathbf{b}/2) = k\pi$. To avoid the large incoherent cross section of hydrogen, we grew 99% deuterated crystals of NENP [17]. Our sample consisted of five crystals with a total mass of 6.54 g mutually aligned to within 25′ in the $(0kl)$ scattering plane. The experiments were performed on the BT4 thermal neutron triple axis spectrometer at the National Institute of Standards and Technology. For energy transfer $\hbar\omega < 5$ meV we fixed the incident neutron energy at 13.7 meV, and used collimations of 22′-22′ and 25′-46′ around the PG(002) monochromator and analyzer, respectively (configuration A). For $\hbar\omega > 5$ meV, the final energy was 13.7 meV, and collimations 22′-22′-25′-46′ (configuration B) or 40′-42′-82′-83′ (configuration C). The data from each configuration were normalized to the integrated intensity of acoustic phonons [18].

Figure 1 shows the ω dependence of the neutron scattering intensity for wave vector transfer $\tilde{q} = 0.7\pi$, 0.5π, and 0.3π at $T = 0.3$ K. We observe sharp peaks superimposed on weakly $\mathbf{Q}$- and ω-dependent incoherent inelastic nuclear scattering. The peaks are identified as inelastic magnetic scattering from the Ni chains because their position depends strongly on $\tilde{q}$ but weakly ($\pm$ 0.2 meV) on the other components of $\mathbf{Q}$, and their intensity versus $|\mathbf{Q}|$ for fixed $\cos\phi = \hat{\mathbf{Q}}\cdot\hat{\mathbf{b}}$ follows the form factor of Ni. Our principal results are evident from this figure: (i) the magnetic scattering is sharply peaked throughout the zone, (ii) constant $\tilde{q}$ scans displaced symmetrically about $\tilde{q} = \pi/2$ have peaks at different energies, and (iii) the energy integrated intensity decreases dramatically for

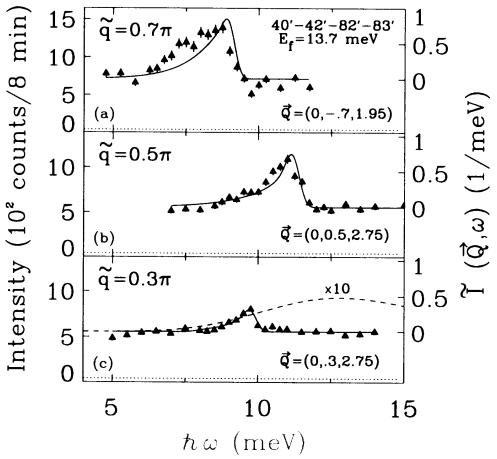

FIG. 1. Constant-**Q** scans for NENP at $T = 0.3$ K. Dashed lines: Background measured with the analyzer turned. Solid lines: Calculated line shapes for infinite-lifetime excitations. Dotted line in (c): Two-magnon intensity calculated from Ref. [13]. Right vertical scale: Absolute units for the magnetic contribution to the scattering intensity $\tilde{I}(\mathbf{Q},\omega) = (1+\cos^2\phi)\tilde{\mathcal{S}}^{\perp}(\tilde{q},\omega)+\sin^2\phi\tilde{\mathcal{S}}^{\parallel}(\tilde{q},\omega)$, where $\tilde{\mathcal{S}}(\tilde{q},\omega)$ is normalized so that $\int\tilde{\mathcal{S}}(\tilde{q},\omega)d\omega = \int\mathcal{S}(\tilde{q},\omega)d\omega = \mathcal{S}(\tilde{q})$.

$\tilde{q} < \pi/2$.

Figure 2 shows the bulk of our data characterizing the low temperature magnetic excitations in NENP. The two peaks at $\tilde{q} = \pi$ lose intensity and merge to a single peak for $\tilde{q} < 0.9\pi$. For $\tilde{q} < 0.5\pi$ the intensity loss for decreasing $\tilde{q}$ is more rapid, until a peak can no longer be discerned for $\tilde{q} < 0.3\pi$. Comparing the typical resolution ellipsoid [19] shown in Fig. 2 to the peak widths, it appears that the peaks are resolution limited. Such resonant modes can be characterized by a dispersion relation $\omega_{\perp,\parallel}(\tilde{q})$ and structure factors $\mathcal{S}^{\perp}_R(\tilde{q}) = \mathcal{S}^{xx}_R(\tilde{q}) = \mathcal{S}^{yy}_R(\tilde{q})$ and $\mathcal{S}^{\parallel}_R(\tilde{q}) = \mathcal{S}^{zz}_R(\tilde{q})$, in terms of which their contribution to the dynamic spin correlation function for $k_BT \ll \hbar\omega_{\perp,\parallel}(\tilde{q})$ can be written [20]

$$\mathcal{S}^{\perp,\parallel}_R(\tilde{q},\omega) = \mathcal{S}^{\perp,\parallel}_R(\tilde{q})\delta(\omega - \omega_{\perp,\parallel}(\tilde{q})) . \quad (2)$$

When the curvature of $\omega_{\perp,\parallel}(\tilde{q})$ is small over the range of the resolution function the positions of peaks in constant-**Q** scans directly yield points on the dispersion relation. In our case, however, it is necessary to take resolution effects into account. This is done by comparing the experimental data to the intensity distribution calculated by inserting a trial dispersion relation in Eq. (2) and convoluting with the known experimental resolution [19]. The simplest dispersion relation that is lattice periodic and adequately fits our data is

$$\omega_{\perp,\parallel}(\tilde{q}) = \sqrt{\Delta^2_{\perp,\parallel} + v^2\sin^2\tilde{q} + A_{\perp,\parallel}\cos^2\frac{\tilde{q}}{2}} . \quad (3)$$

The solid lines in Figs. 1 and 2 are the result of a global fit of Eq. (3) to all our data. Apart from the parameters in $\omega(\tilde{q})$, only $\mathcal{S}^{\perp,\parallel}_R(\tilde{q})$ and a flat background were varied for each constant-**Q** scan [21]. The good overall agreement between model and data ($\chi^2 = 2.6$) indicates that Eq. (3) provides an adequate description of the dispersion relation for $\tilde{q} \geq 0.3\pi$, and that the broadening of the peaks is a resolution effect. To set a lower limit for the lifetime τ of these modes, we replaced the δ functions in Eq. (2) by Gaussians with full width at half maximum $1/\tau$, and determined the experimental lower limit on τ as the value at which the reduced χ^2 increases by 30%. In this way we found $\omega(\tilde{q})\tau > 10$ for $0.3\pi \leq \tilde{q} \leq \pi$.

The dispersion relation extracted from this analysis is shown in Fig. 3(a). Alternatively we show data points obtained by fitting resolution-corrected line shapes based on Eq. (3) to each constant-**Q** scan. The fact that these points cluster about the dispersion relation proves that our analysis is not biased by the choice of Eq. (3). Apart from displaying the Haldane gap, the dispersion relation

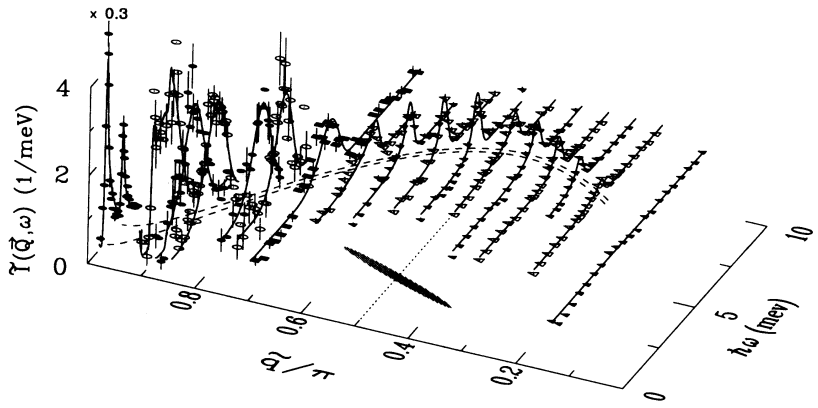

FIG. 2. Normalized magnetic scattering intensity from NENP at $T = 0.3$ K. Solid lines: Calculated intensity profiles for infinite-lifetime excitations based on the dispersion relation shown with a dashed line [Eq. (3)]. Throughout we use circles, squares, and triangles for data from configurations A, B, and C, respectively. The ellipsoid is FWHM of the resolution for $\tilde{q} = 0.5\pi$. Data at $\tilde{q} = 0.975\pi, 0.85\pi$, and 0.25π have been omitted for clarity.

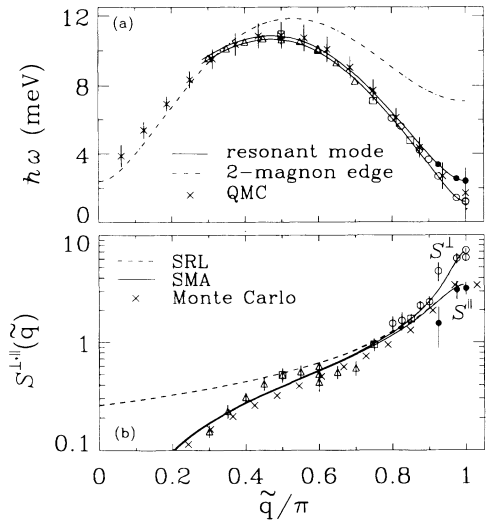

FIG. 3. (a) Circles, triangles, squares, and solid lines: Experimental dispersion relation $\omega(\tilde{q})$ of long-lived modes in NENP. Error bars are smaller than the symbol size. Dot-dashed line: Lower edge of corresponding two-magnon continuum. Crosses: QMC results [12] scaled by $J = 4.1$ meV. (b) Instantaneous spin correlation function $\mathcal{S}^{\perp,\parallel}(\tilde{q})$. Crosses: Monte Carlo results [30]. Dashed lines: Square-root Lorentzians with $\xi = 8.5$ and 4.2. Solid lines: Single mode approximation based on $\omega(\tilde{q})$. In both (a) and (b), open and solid symbols for $\tilde{q} > 0.9\pi$ correspond to polarizations perpendicular and parallel to the chain.

is anomalous in having a bandwidth of 11 meV which is 1.4 times the prediction of classical spin wave theory, $2JS = 8$ meV. For comparison the highest energy resonant mode in the $S = 1/2$ case occurs at $\pi/2$ times $2JS$. The most interesting characteristic of $\omega_{\perp,\parallel}(\tilde{q})$, however, is the asymmetry of the dispersion relation about $\tilde{q} = \pi/2$. For conventional Néel antiferromagnets the unit cell is doubled and $\tilde{q} = \pi/2$ is a point on the Brillouin zone boundary of high symmetry for spin wave dispersion relations. From Fig. 3(a) this is clearly not the case for NENP. We conclude that the ground state of this material retains the full translational symmetry of the lattice.

Although we do not wish to put undue emphasis on the functional form of the dispersion relation used in our analysis [Eq. (3)], it provides a convenient framework within which to compare our data to existing theories. The optimal parameters obtained from our analysis are $\Delta_\perp = 1.19(5)$ meV and $\Delta_\parallel = 2.40(5)$ meV, consistent with previous experiments [4], and $v = 9.7(1)$ meV, $A_\perp = A_\parallel = 34(2)$ meV^2. Conventional spin wave theories yield dispersion relations identical to Eq. (3), with the constraint $A_{\perp,\parallel} = \pm(\Delta_\parallel^2 - \Delta_\perp^2)$ [22], clearly inconsistent with our results. More relevantly Gómez-Santos [23] derived by a variational approach a dispersion relation for the isotropic $S = 1$ chain identical to Eq. (3), but with parameters inconsistent with our experiment.

Numerical simulations on finite size chains have obtained results consistent with ours [12, 24]. Figure 3(a) also shows Takahashi's quantum Monte Carlo (QMC) result [12] for the lowest energy excited state (LEES) of the isotropic $S = 1$ chain, scaled by $J = 4.1$ meV. Although detailed comparison with data for NENP at $\tilde{q} = \pi$ is not possible, it appears that for $\tilde{q} > 0.3\pi$ the LEES coincides with the long-lived mode that we observe. For $\tilde{q} < 0.3\pi$ the LEES falls below the extrapolated dispersion relation, and follows closely the lower edge of the two-magnon continuum generated from our measured dispersion relation [dash-dotted line in Fig. 3(a)].

In view of the dominant role played by the multimagnon continuum in the $S = 1/2$ case [25, 26] it is important to understand its contribution to $\mathcal{S}(\tilde{q},\omega)$ for $S = 1$. Although we did not directly observe multimagnon scattering, the total moment sum rule $(1/L)\sum_{\alpha,\tilde{q}} \mathcal{S}^{\alpha\alpha}(\tilde{q}) = S(S+1)$ allows us to set an upper bound on its contribution to $\mathcal{S}(\tilde{q},\omega)$. Figure 3(b) shows our result for the structure factor of the resonant mode, $\mathcal{S}_R^{\alpha\alpha}(\tilde{q})$, extracted by the global least squares analysis. Summing these data, we obtain $2.6(6) \simeq S(S+1)$ implying that within error resonant excitations alone exhaust the sum rule. This excludes a large static ordered moment in NENP at 0.3 K [27], and proves that multimagnon excitations carry little spectral weight for the $S = 1$ chain [24].

Because it is the Fourier transform of the instantaneous spin correlation function $\langle S_0^\alpha S_\ell^\alpha \rangle$, $\mathcal{S}^{\alpha\alpha}(\tilde{q})$ is central to the characterization of the ground state. For the integer spin isotropic [1] and the $S = 1$ anisotropic [28] cases, theory predicts that $\langle S_0^\alpha S_\ell^\alpha \rangle \sim (-1)^\ell \ell^{-1/2} \exp(-\ell/\xi)$ for $\ell/\xi \gg 1$. This implies that $\mathcal{S}^{\alpha\alpha}(\tilde{q}) \propto \{1 + [(\tilde{q}-\pi)\xi]^2\}^{-1/2}$ for $(\tilde{q}-\pi)\xi \ll 1$. This square-root Lorentzian (SRL) [10, 29], shown as a dashed line in Fig. 3(b), is consistent with our data for $|\tilde{q}-\pi| < 0.2\pi$, but beyond this regime the SRL decreases more slowly than $\mathcal{S}(\tilde{q})$ because near-neighbor correlations are overestimated by the continuum theory. The crosses show Monte Carlo results for a 64 spin chain [30] which are in qualitative agreement with our data, although detailed comparison near $\tilde{q} = \pi$ is precluded by the single ion anisotropy of NENP.

The results that $\mathcal{S}(\tilde{q},\omega) \simeq \mathcal{S}_R(\tilde{q},\omega)$ and $\omega(\tilde{q})\tau \gg 1$ for all $\tilde{q}$ with significant spectral density allow us to use the SMA [11, 25, 31] to relate $\mathcal{S}^{\alpha\alpha}(\tilde{q})$ to $\omega_{\perp,\parallel}(\tilde{q})$:

$$\mathcal{S}^{\alpha\alpha}(\tilde{q}) \simeq \frac{1}{\omega^{\alpha\alpha}(\tilde{q})} \int_{-\infty}^{\infty} \omega \mathcal{S}^{\alpha\alpha}(\tilde{q},\omega) d\omega \tag{4}$$

$$\simeq -\frac{2}{3} \frac{\langle \mathcal{H} \rangle / L}{\hbar\omega^{\alpha\alpha}(\tilde{q})} (1 - \cos\tilde{q}) , \tag{5}$$

where $\langle \mathcal{H} \rangle / L$ is the ground state energy per spin. The solid lines in Fig. 3(b) are a one-parameter fit using Eq. (5) and our measured dispersion relation. This yields $\langle \mathcal{H} \rangle / JL = -1.5(4)$, indistinguishable from the value -1.4 obtained by Monte Carlo simulation [30]. For $\tilde{q} \sim \pi$ Eq. (5) becomes a SRL with $\xi_{\perp,\parallel} = \Delta_{\perp,\parallel}^{-1} \sqrt{v^2 + A_{\perp,\parallel}}/4$, resulting in values of 8.5(4) and 4.2(1) for the transverse and parallel dynamic correlation lengths.

In the low-$\tilde{q}$ regime, the fact that we do not discern a peak for $\tilde{q} < 0.3\pi$ is consistent with the intensity predicted by the SMA, but leaves open the question of whether or not the resonant mode survives within the two-magnon continuum (Fig. 3). Affleck and Weston [13] have calculated the two-magnon contribution to $\mathcal{S}(\tilde{q},\omega)$ in the $\tilde{q} \simeq 0$ limit for $S = 1$ chains using a Ginzburg-Landau approach to treat the finite anisotropy appropriate for NENP. With our measured parameters, this model predicts a two-magnon contribution to the total moment sum rule of 0.083 for $|\tilde{q}| \leq 0.3\pi$, consistent with our conclusion that one-magnon modes dominate the fluctuations. Upon convolution of Eq. (4.3) of Ref. [13] with our experimental resolution function at $\tilde{q} = 0.3\pi$ this theory predicts the weak, broad peak shown magnified 10 times in Fig. 1(c). Although the integrated intensities of the measured resonant mode and the theoretical two-magnon spectrum are comparable at this $\tilde{q}$, the latter cannot be separated from the strong incoherent inelastic nuclear scattering.

To put our results into context we mention that a diverse class of quantum systems that do not break translational symmetry in their ground states have excitations that are well described by the SMA. These include superfluid ^{4}He, the two-dimensional electron gas in the fractional quantum Hall regime, and the bilinear-biquadratic (AKLT) spin chain [11, 32], although only for ^{4}He do direct measurements of the excitation spectrum exist. Our results indicate that as anticipated [11], the pure bilinear chain also falls in this class. Recall that in ^{4}He the roton minimum in the dispersion relation results from short-range correlations in the liquid. Analogously, but with the important difference that $\mathcal{S}^{\alpha\alpha}(\tilde{q} = 0) = 0$, the decrease in the excitation energy that occurs for $\tilde{q} < \pi/2$ in NENP but not in the AKLT chain [11] suggests the closer proximity of the former system to Néel order which would enforce π periodicity in $\omega(\tilde{q})$.

It is a pleasure to thank M. Kaplan for information on the growth of NENP, G. Aeppli, I. Affleck , S. Geschwind, D. Huse, L. Lévy, P. A. Lindgård, A. M. Tsvelik, and Y. J. Uemura for helpful discussions, and R. Lindstrom and R. Paul for performing the neutron activation analysis. C.B. and D.H.R. thank the Aspen Center for Physics where some of this work was performed.

[a] Present address: Brookhaven National Laboratory, Upton, NY 11973.

[1] F. D. M. Haldane, Phys. Lett. **93A**, 464 (1983); Phys. Rev. Lett. **50**, 1153 (1983).
[2] M. P. Nightingale and H. W. J. Blöte, Phys. Rev. B **33**, 659 (1986).
[3] Z. Tun *et al.*, Phys. Rev. B **42**, 4677 (1990), and references therein.
[4] L. P. Regnault *et al.*, Physica (Amsterdam) **156-157B**, 247 (1989), and references therein.
[5] K. Katsumata *et al.*, Phys. Rev. Lett. **63**, 86 (1989).
[6] Y. Anjiro *et al.*, Phys. Rev. Lett. **63**, 1424 (1989).
[7] M. Date and K. Kindo, Phys. Rev. Lett. **65**, 1659 (1990).
[8] M. Hagiwara *et al.*, Phys. Rev. Lett. **65**, 3181 (1990).
[9] S. H. Glarum *et al.*, Phys. Rev. Lett. **67**, 1614 (1991).
[10] H. Mutka *et al.*, Phys. Rev. Lett. **67**, 497 (1991).
[11] D. P. Arovas, A. Auerbach, and F. D. M. Haldane, Phys. Rev. Lett. **60**, 531 (1988).
[12] M. Takahashi, Phys. Rev. Lett. **62**, 2313 (1989).
[13] I. Affleck and R. A. Weston, Phys. Rev. B **45**, 4667 (1992). In this paper, $\mathcal{S}(\tilde{q},\omega)$ [Eq. (2.6)] should have prefactor $1/v$, not $1/v^2$. All subsequent formulas should be suitably modified.
[14] A. Meyer *et al.*, Inorg. Chem. **21**, 1729 (1982).
[15] T. Delica, K. Kopinga, H. Leschke, and K. K. Mon, Europhys. Lett. **15**, 55 (1991).
[16] L. P. Regnault, C. Vettier, J. Rossat-Mignod, and J. P. Renard (unpublished).
[17] H and D concentrations were determined by prompt γ-ray neutron activation analysis performed at the National Institute of Standards and Technology.
[18] The systematic error in this procedure is approximately 25% resulting from incomplete knowledge of the phonon polarization vectors and the low temperature structure.
[19] N. D. Chesser and J. D. Axe, Acta Crystallogr. Sect. A **29**, 160 (1973).
[20] Here we have made the additional simplification of assigning a fixed polarization to each mode. For $\tilde{q} > 0.9\pi$ where the two modes are resolved this is a good approximation.
[21] We fixed $A_\perp = A_\parallel$ and for $\tilde{q} \leq 0.9\pi$ where we did not resolve the two modes, we fixed $\mathcal{S}_R^\perp(\tilde{q}) = \mathcal{S}_R^\parallel(\tilde{q})$.
[22] $\Delta_\perp = \Delta_\parallel = 0$ for the Heisenberg case, $\Delta_\perp = 0$ for the x-y case, and $\Delta_\perp = \Delta_\parallel$ for the Ising case.
[23] G. Gómez-Santos, Phys. Rev. Lett. **63**, 790 (1989).
[24] J. Deisz, M. Jarrell, and D. L. Cox, Phys. Rev. B **42**, 4869 (1990); J. Deisz, Ph.D. thesis, The Ohio State University, 1991 (unpublished); S. V. Meshkov (to be published).
[25] G. Müller, H. Thomas, M. W. Puga, and H. Beck, J. Phys. C **14**, 3399 (1981).
[26] I. U. Heilmann *et al.*, Phys. Rev. B **18**, 3530 (1978); S. E. Nagler *et al.*, Phys. Rev. B **44**, 12361 (1991).
[27] B. J. Sternlieb *et al.*, J. Magn. Magn. Mater. **104-107**, 801 (1992), find by μ^+ spin rotation a small component of quasielastic magnetic fluctuations for $T < 3$ K in NENP.
[28] A. M. Tsvelik, Phys. Rev. B **42**, 10499 (1990).
[29] L. P. Regnault, J. Rossat-Mignod, and J. P. Renard, J. Magn. Magn. Mater. **104-107**, 869 (1992).
[30] K. Nomura, Phys. Rev. B **40**, 2421 (1989); S. Liang, Phys. Rev. Lett. **64**, 1597 (1990), obtains similar results.
[31] P. C. Hohenberg and W. F. Brinkman, Phys. Rev. B **10**, 128 (1974).
[32] S. M. Girvin, A. H. MacDonald, and P. M. Platzman, Phys. Rev. B **33**, 2481 (1986).

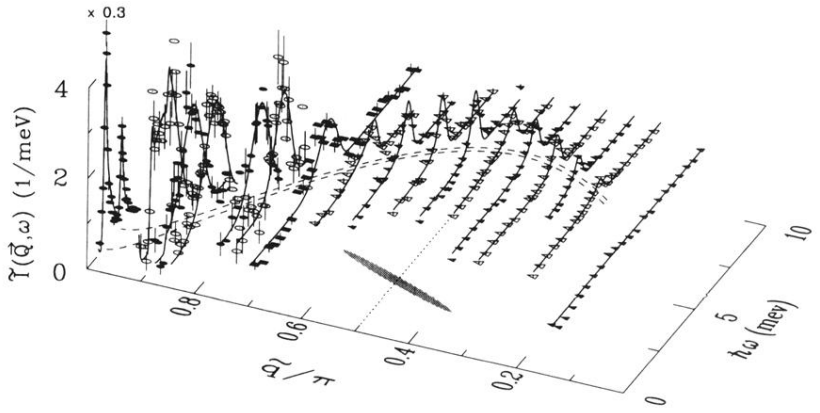

FIG. 2. Normalized magnetic scattering intensity from NENP at $T = 0.3$ K. Solid lines: Calculated intensity profiles for infinite-lifetime excitations based on the dispersion relation shown with a dashed line [Eq. (3)]. Throughout we use circles, squares, and triangles for data from configurations A, B, and C, respectively. The ellipsoid is FWHM of the resolution for $\tilde{q} = 0.5\pi$. Data at $\tilde{q} = 0.975\pi, 0.85\pi$, and 0.25π have been omitted for clarity.